Mathematical Biosciences and Engineering

Research article

Bifurcations in a discontinuous Leslie-Gower model with harvesting and alternative food for predators and constant prey refuge at low density

Christian Cortés García[1,2,*]

[1] Department of Mathematics, Universidad Carlos III de Madrid, 30 University Avenue, Madrid, Spain

[2] Department of Systems Biology, Centro Nacional de Biotecnología, 3 Darwin Street, Madrid, Spain

* **Correspondence:** Email: chcortes@math.uc3m.es, cc.cortes@cnb.csic.es.

Abstract: Since environmental studies have shown that a constant quantity of prey become refuges from the predator at low densities and become accessible again for consumption when they reach a higher density, in this work we propose a discontinuous mathematical model, Lesli-Gower type, which describes the dynamics between prey and predators, interacting under the same environment, and whose predator functional response, of linear type, is altered by a refuge constant in the prey when below a critical value. Assuming that predators can be captured and have alternative food, the qualitative analysis of the proposed discontinuous model is performed by analyzing each of the vector fields that compose it, which serves as the basis for the calculation of the bifurcation curves of the discontinuous model, with respect to the threshold value of the prey and the harvest rate of predators. It is concluded that the perturbations of the parameters of the model leads either to the extinction of the predators or to a stabilization in the growth of both species, regardless of their initial conditions.

Keywords: filippov systems; threshold value; bifurcation analysis; logistic growth; pseudo-equilibrium

1. Introduction

The behavior between two species, predator and prey coexisting in the same environment, is a subject of study in ecology and several researchers have proposed mathematical models that describe the dynamics of both species. These models are usually described by systems of continuous ordinary differential equations

$$\dot{u} = f(u, \alpha), \tag{1.1}$$

where $u \in \mathbb{R}^2$ is the size for each population, measured in number of individuals or density per unit area or volume at any instant $t \geq 0$, $\alpha \in \mathbb{R}^p$, with $p \geq 1$ and non-negative inputs, a vector of parameters and

$f : \Omega \subset \mathbb{R}^2 \times \mathbb{R}^p \to \mathbb{R}^2$ a continuous and differentiable function. The qualitative analysis of the model (1.1) determines the conditions in its parameters to achieve a possible stabilization in both species, or an extinction of at least one of them. This process is called *bifurcation*, where its possible cases were listed in [1].

In particular, Leslie-Gower models have been used to describe the dynamics of both species, which assumes that, in addition to the carrying capacity of the environment for the intrinsic growth of prey, the environmental carrying capacity in predators should be proportional to the abundance of prey [2]. However, several researchers have made modifications to the Leslie-Gower model, considering, for example, alternative food for predators, various functions describing the predator functional response, or harvesting for one or both species [3–7].

In the simplest case, if $x(t), y(t) \geq 0$ are the population sizes of prey and predators, respectively, whitch prey growth is subject to the carrying capacity of the environment $K > 0$ and, the growth of predators under the quality of the utilization of consumed prey $n > 0$ and of the possible alternative food available $c > 0$ in the environment for new births, the dynamics of prey $x(t)$ and predators $y(t)$ is given by:

$$W(x,y) : \begin{cases} \dot{x} &= rx\left(1 - \dfrac{x}{K}\right) - axy \\ \dot{y} &= sy\left(1 - \dfrac{y}{nx + c}\right) - qEy, \end{cases} \tag{1.2}$$

where $r, s > 0$ are the intrinsic growth rates of prey and predators, respectively, $q > 0$ is the harvest coefficient, $E > 0$ the harvest effort, and $a > 0$ the hunting success rate of the predator affecting the prey. In this case, it is assumed that predators can consume the prey without any limitation or resistance, so the predator functional response is linear [8], that is, $h(x) = ax$.

On the other hand, the effort of prey refuge from predators could play an important role in the stabilization of an ecological system, which generates an additional interest on the part of ecologists, and of which the effect of the reduction in the quantity of prey that will not be consumed by the predator is analyzed with respect to the different dynamics that could be presented by the model proposed.

In general, there are two types of prey refuge: the quantity of refuge is proportional to the population size of the prey [9–11] or it is a fixed quantity [12, 13]. However, the qualitative analysis in predator-prey models when considering a proportion of refuged prey is equivalent to the model with no refuge [9, 10], as opposed to considering a fixed quantity of refuge in the prey [14]. In particular, if $0 < m < K$ denotes a fixed quantity of refuge for the prey, the model (1.2) is modified by:

$$X(x,y) : \begin{cases} \dot{x} &= rx\left(1 - \dfrac{x}{K}\right) - a(x - m)y \\ \dot{y} &= sy\left[1 - \dfrac{y}{n(x - m) + c}\right] - qEy, \end{cases} \tag{1.3}$$

where the initial prey condition $x(0)$ must be greater than m, that is, $m < x(0) \leq K$.

However, if $x(0) \leq m$, prey and predators do not interact in the environment, so predators must feed only on resources provided by the environment and the growth of both species must be modeled by logistic differential equations of the form

$$Y(x,y) : \begin{cases} \dot{x} &= rx\left(1 - \dfrac{x}{K}\right) \\ \dot{y} &= sy\left(1 - \dfrac{y}{c}\right) - qEy. \end{cases} \tag{1.4}$$

In particular, the model (1.3) for $m < x \leq K$ and the model (1.4) for $0 \leq x \leq m$ can be generalized by systems of discontinuous differential equations, generally known as Filippov's planar systems [15, 16], described by

$$
\begin{cases}
\dot{u} & = & f_1(u, \alpha), & u \in S_1, \\
& \vdots & \\
\dot{u} & = & f_k(u, \alpha), & u \in S_k,
\end{cases}
\tag{1.5}
$$

where $f_i : S_i \times \mathbb{R}^p \to \mathbb{R}^2$, with $1 \leq i \leq k$, are continuous functions in an open and non-overlapping region S_i, separated from S_j by a differentiable curve Σ_{ij}. The discontinuous models (1.5) are called *Filippov systems*, whose bifurcation cases, which in addition to the possible cases shown in [1] for vector fields f_i, were listed by Kuznetsov [15].

In addition, since there are species, such as cardumens [17, 18], that hide from the predator when their population size is critical, so that the predator is forced to change its diet to avoid extinction [19–21], and when the desired population size is exceeded again, they leave their hiding place to search for food or explore the environment, and become accessible to the predator again [22–24], researchers have focused additional interest in proposing mathematical models that describe such interaction between prey and predators, when the predator functional response is deactivated if the population size of prey is below a threshold value $M > 0$ [25–29].

However, and in contrast to discontinuous models proposed [25–29], by assuming that there are a quantity of prey that do not hide from the predator when it is below its critical population size $M > 0$, for example, because they move away from other species to explore the environment undetected, we are interested in analyzing the behavior between prey and predators when a fixed quantity of prey $m > 0$ is protected by being below its critical value $M > 0$. Therefore, and given that there are species with a linear predator functional response [8, 30], in this paper we propose, and perform a local and global qualitative analysis, a discontinuous Lesli-Gower model of the form,

$$
V(x, y) : \begin{cases}
\dot{x} & = & rx\left(1 - \dfrac{x}{K}\right) - a(x - \epsilon m)y \\
\dot{y} & = & sy\left[1 - \dfrac{y}{n(x - \epsilon m) + c}\right] - qEy,
\end{cases}
\tag{1.6}
$$

where

$$
\epsilon = \begin{cases}
0, & \text{if} & x > M, \\
1, & \text{if} & m < x < M, \\
\frac{x}{m} & \text{if} & x < m,
\end{cases}
$$

and $0 < m < M < K$. In this case, if $m < x < M$ then the prey is protected by a refuge constant $m > 0$, and from which they become accessible to the predator if $x > M$. However, if $x < m$, prey are totally protected from the predator, so predators must subsist on alternative food provided by the environment.

For this purpose, the Section 2 presents the necessary tools to carry out a qualitative analysis of a Filippov system [15, 16, 28, 29]. In Sections 3–5, a qualitative and bifurcation analysis is performed on the models (1.3), when $m \in (0, K)$ and $m = 0$, and (1.4) respectively, and whose results are used to perform the local and global analysis of the Filippov systems (1.6), shown in Section 6. A contrast to the Filippov systems (1.6) is performed with a bifurcation analysis with respect to the parameters $M, E > 0$.

2. Preliminaries

Let a planar Filippov system $Z = (X, Y)$ a vector field in an open set $U \subset \mathbb{R}^2$ defined by

$$Z(x, y) = \begin{cases} X(x, y), & (x, y) \in \Sigma^+ \\ Y(x, y), & (x, y) \in \Sigma^-, \end{cases}$$

where X, Y are vector fields of class C^r, with $r > 1$, and $\Sigma = \{(x, y) \in U : f(x, y) = 0, \operatorname{grad} f(x, y) \neq 0\}$, with $f : U \to \mathbb{R}$ a function of class C^r, is a differentiable curve that divides U into two open regions

$$\Sigma^+ = \{(x, y) \in U : f(x, y) > 0\} \quad \text{and} \quad \Sigma^- = \{(x, y) \in U : f(x, y) < 0\}.$$

If $p = (x, y) \in \Sigma^+$, the local trajectory $\varphi_Z(t, p)$ in $Z = (X, Y)$, with initial point in p, is defined by trajectory $\varphi_X(t, p)$ in the vector fields X. Analogously, if $p = (x, y) \in \Sigma^-$, then $\varphi_Z(t, p) = \varphi_Y(t, p)$, where $\varphi_Y(t, p)$ is the trajectory in the vector fields Y.

However, a trajectory $\varphi_Z(t, p)$ must also be defined for $p = (x, y) \in \Sigma$. The following result determines a division of Σ that depends on the behavior of the vector fields X and Y.

Definition 1. *Let $Xf(p) = \langle X(p), \operatorname{grad} f(p) \rangle$ and $Yf(p) = \langle Y(p), \operatorname{grad} f(p) \rangle$, with $p = (x, y) \in \Sigma$, then Σ is divided into three disjoint regions given by:*

- *Crossing region: $\Sigma^c = \{p \in \Sigma : Xf(p) \cdot Yf(p) > 0\}$,*
- *Sliding region: $\Sigma^s = \{p \in \Sigma : Xf(p) < 0, Yf(p) > 0\}$,*
- *Escaping region: $\Sigma^e = \{p \in \Sigma : Xf(p) > 0, Yf(p) < 0\}$.*

By the Definition 1, for the case in which there exists $p \in \Sigma$ such that $Xf(p) = 0$ or $Yf(p) = 0$, the following result defines the tangent point at $Z = (X, Y)$.

Definition 2. *If $p \in \partial\Sigma^c \cup \partial\Sigma^s \cup \partial\Sigma^e$ such that $Xf(p) = 0$ or $Yf(p) = 0$, where $\partial\Sigma^{c,e,s}$ are the boundaries of the regions $\Sigma^{c,e,s}$, the point p is called tangency point, and it can be classified as:*

- *quadratic if $Xf(p) = 0$ and $X^2f(p) = \langle X(p), \operatorname{grad}Xf(p) \rangle \neq 0$, or $Yf(p) = 0$ and $Y^2f(p) = \langle Y(p), \operatorname{grad}Yf(p) \rangle \neq 0$. A quadratic tangency $p \in \Sigma$ is regular if $Xf(p) = 0$, $X^2f(p) \neq 0$ and $Yf(p) \neq 0$; or $Yf(p) = 0$, $Y^2f(p) \neq 0$ and $Xf(p) \neq 0$. For the first case, a regular quadratic tangency is visible if $X^2f(p) > 0$ and invisible if $X^2f(p) < 0$. For the second case, $p \in \Sigma$ is visible if $Y^2f(p) < 0$ and invisible if $Y^2f(p) > 0$.*
- *cubic if $Xf(p) = X^2f(p) = 0$ and $X^3f(p) = \langle X(p), \operatorname{grad}X^2f(p) \rangle \neq 0$ or $Yf(p) = Y^2f(p) = 0$ and $Y^3f(p) = \langle Y(p), \operatorname{grad}Y^2f(p) \rangle \neq 0$.*

We will now define the trajectory $\varphi_Z(t, p)$ for a initial point p in Σ^c, Σ^s or Σ^e. According to Filippov's method [15, 16, 28, 29], the trajectory $\varphi_Z(t, p)$ with $p \in \Sigma^s \cup \Sigma^e$ is given by a convex combination of the vector fields X and Y tangent to Σ, that is,

$$Z^s(p) = \lambda(p)X(p) + [1 - \lambda(p)]Y(p).$$

In view of the Figure 1, the *sliding vector field Z^s* is defined below.
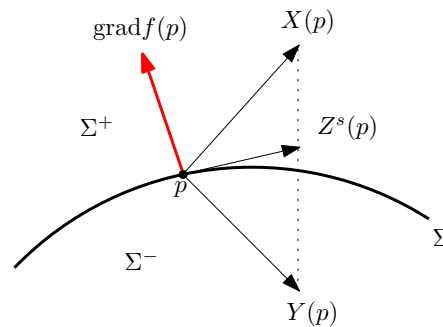
Figure 1. Construction of trajectories $Z^s(p)$.

**Definition 3.** *The sliding vector field Z^s is given by*

$$Z^s(p) = \frac{Yf(p)X(p) - Xf(p)Y(p)}{Yf(p) - Xf(p)}, \tag{2.1}$$

defined in $\Sigma^e \cup \Sigma^s$. For $p \in \Sigma^e \cup \Sigma^s$, the local trajectory $\varphi_Z(t, p)$ of p is given by this vector field. The point $p \in \Sigma^s \cup \Sigma^e$ is called pseudo-equilibrium if $Z^s(p) = 0$.

Keeping in mind this background, the trajectory $\varphi_Z(t, p)$ in $Z = (X, Y)$ is defined as follows.

Definition 4. *Let φ_X and φ_Y the trajectories in the vector fields X and Y defined for $t \subset I \in \mathbb{R}$, respectively. The local trajectory φ_Z in $Z = (X, Y)$ through a point p is defined as follows:*

- *For $p \in \Sigma^+$ or $p \in \Sigma^-$ such that $X(p) \neq 0$ or $Y(p) \neq 0$ respectively, the trajectory is given by $\varphi_Z(t, p) = \varphi_X(t, p)$ or $\varphi_Z(t, p) = \varphi_X(t, p)$ respectively, for $t \subset I \in \mathbb{R}$.*
- *For $p \in \Sigma^c$ such that $Xf(p), Yf(p) > 0$, and taking the origin of time at p, the trajectory is defined as $\varphi_Z(t, p) = \varphi_Y(t, p)$ for $t \subset I \cap \{t \leq 0\}$ and $\varphi_Z(t, p) = \varphi_X(t, p)$ for $t \subset I \cap \{t \geq 0\}$. For the case $Xf(p), Yf(p) < 0$, the trajectory is defined as $\varphi_Z(t, p) = \varphi_Y(t, p)$ for $t \subset I \cap \{t \geq 0\}$ and $\varphi_Z(t, p) = \varphi_X(t, p)$ for $t \subset I \cap \{t \leq 0\}$.*
- *For $p \in \Sigma^e \cup \Sigma^s$ such that $Z^s(p) \neq 0$, the trajectory is given by $\varphi_Z(t, p) = \varphi_{Z^s}(t, p)$ for $t \in I \subset \mathbb{R}$, where Z^s is the sliding vector field given in (2.1).*
- *For $p \in \partial\Sigma^c \cup \partial\Sigma^s \cup \partial\Sigma^e$ such that the definitions of trajectories for points in Σ in both sides of p can be extended to p and coincide, the trajectory through p is this common trajectory. We will call these points regular tangency points.*
- *For any other point $\varphi_Z(t, p) = \{p\}$ for all $t \in I \subset \mathbb{R}$. This is the case of the tangency points in Σ which are not regular and which will be called singular tangency points and are the critical points of X in Σ^+, Y in Σ^- and Z^s in $\Sigma^e \cup \Sigma^s$.*
- *As observed in Figure 2(a), a regular periodic trajectory is a trajectory $\Gamma = \{\varphi_Z(t, p) : t \in \mathbb{R}\}$, which therefore belongs to $\Sigma^+ \cup \Sigma^- \cup \overline{\Sigma^c}$ such that $\varphi_Z(t + T, p) = \varphi_Z(t, p)$ for some $T > 0$.*
- *A limit cycle in Σ^+, or in Σ^-, is a limit cycle in $Z = (X, Y)$ which is represented in Figure 2(b).*
- *A cycle in $Z = (X, Y)$ is a limit cycle formed by the union of a sequence of curves $\gamma_1, \cdots, \gamma_n$, such that $\gamma_{2k} \subset \Sigma^s$ and $\gamma_{2k+1} \subset \Sigma^+ \cup \Sigma^-$, where the arrival and departure points belong to the closures of γ_{2k} and γ_{2k+1}, respectively. Figure 2(c) is an example of a cycle where $n = 2$.*
- *A pseudo-cycle is the union of a set of trajectories $\gamma_1, \cdots, \gamma_n$, contained in Σ^+ or Σ^-, such that the end point of some γ_i coincides with the end point of the next curve and the initial point of γ_i coincides with the initial point of the previous curve. Figure 2(d) shows a pseudo-cycle.*
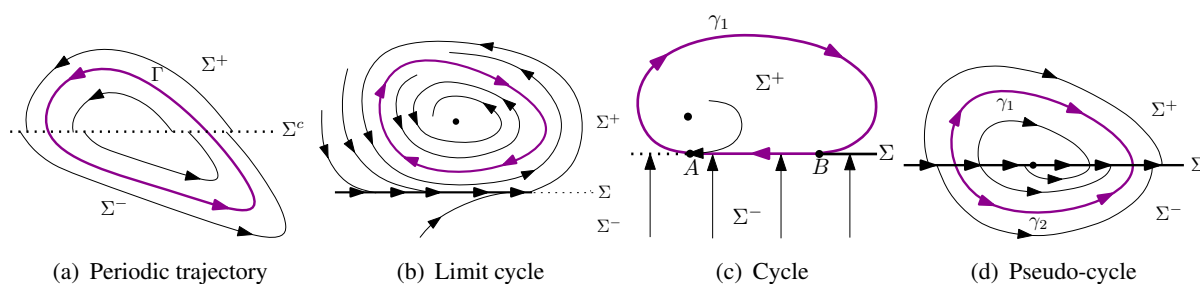
Figure 2. Examples of a periodic orbit, limit cycle, cycle, and a pseudo-cycle in $Z = (X, Y)$ represented by the purple curve. The black curves are trajectories that are not periodic.

With the basic notions for Filippov systems, we can perform the qualitative analysis for the model (1.6). For this purpose, the qualitative analysis of the vector fields W, X and Y will be performed, the results of which are used to analyze the dynamics of the discontinuos model (1.6), where the discontinuity in the vector fields W and X will be analyzed, and subsequently the discontinuity of X and Y.

3. Prey refuge model

Let $x(t) \geq 0$ and $y(t) \geq 0$ the population sizes of prey and predator, respectively, whose dynamics are represented by the model (1.3) and defined in the region of biological sense

$$\Omega_m = \left\{(x, y) \in \mathbb{R}^2 : m \leq x \leq K, 0 \leq y \leq n(K - m) + c\right\}.$$

Before performing a mathematical analysis to determine possible behaviors in the dynamics of prey and predators, one must verify that the model (1.3) is mathematically correct and biologically feasible. Indeed,

Lemma 1. *The model (1.3) has a unique trajectory φ_X, with initial condition $(x(0), y(0)) \in \Omega_m$. Moreover, Ω_m is invariant.*

Proof. Since the vector field (1.3) is continuously differentiable for all $(x, y) \in \Omega_m$, the existence and uniqueness of the trajectory φ_X is satisfied. On the other hand, it must be guaranteed that the trajectories φ_X of the model (2.1) do not escape from Ω_m. For this purpose, the change in the trajectories φ_X of the model (1.3) on the boundary is analyzed. Indeed, if $x = m$ then $\dot{x} = rm\left(1 - \frac{m}{K}\right) \geq 0$ for all $y \geq 0$. Similarly, if $x = K$ then $\dot{x} = -a(K - m)y \leq 0$ for all $y \geq 0$. On the other hand, if $y = 0$ then $\dot{y} = 0$ for all $x \geq 0$. If $y = n(K - m) + c$, we have that $\dot{y} \leq -qE[n(K - m) + c] \leq 0$ for all $0 \leq x \leq K$. Therefore, the trajectories φ_X do not cross the boundary of Ω_m.

Lemma 2. *The trajectories φ_X of the model (1.3) are uniformly bounded.*

Proof. Note that

$$\dot{x} = rx\left(1 - \frac{x}{K}\right) - a(x - m)y \leq rx\left(1 - \frac{x}{K}\right),$$

which corresponds to a logistic differential equation, that is,

$$x(t) \leq \frac{Kx(0)e^{rt}}{K + x(0)(e^{rt} - 1)},$$

with $x(0) \in \Omega_m$ the initial condition of the solution $x(t)$. Consequently, $x(t) \leq K$ for all $t \geq 0$.

On the other hand, note that,

$$\dot{y} = sy\left[1 - \frac{y}{n(x-m)+c}\right] - qEy \leq sy\left[1 - \frac{y}{n(K-m)+c}\right].$$

If $S = n(K-m) + c$, we have that $y(t) \leq S$. Thus, when considering the function $W(t) : \mathbb{R}_+ \to \mathbb{R}_+$ given by

$$W(t) = x(t) + y(t)$$

then $0 \leq W(t) \leq K + S$ and the trajectories φ_X of the model (1.3) are uniformly bounded.

3.1. Local and global qualitative analysis

The equilibrium in the model (1.3) on the x-axis is given by $P_1 = (K, 0) \in \Omega_m$. Moreover, the model (1.3) could have a maximum of two interior equilibriums $P_{3,4} = (x_{1,2}, y_{1,2})$, with

$$y_{1,2} = \frac{(s - qE)(nx_{1,2} + c - mn)}{s}, \tag{3.1}$$

and $x_{1,2}$ as positive solutions of the polynomial $Ax^2 + Bx + C = 0$, with

$$\begin{aligned} A &= rs + aKn(s - qE), \\ B &= aK(c - 2mn)(s - qE) - rsK, \\ C &= -aKm(c - mn)(s - qE), \end{aligned} \tag{3.2}$$

that is,

$$x_{1,2} = \frac{-B \pm \sqrt{B^2 - 4AC}}{2A}. \tag{3.3}$$

To determine the number of interior equilibrium, we proceed by analyzing the following cases.

- Case $c - mn > 0$: If $s - qE \leq 0$, the model (1.3) does not exhibit interior equilibriums, since $y_{1,2} < 0$. If $s - qE > 0$, then $A > 0$ and $C < 0$, so the model (1.3) has an interior equilibrium $P_3 = (x_1, y_1)$.
- Case $c - mn = 0$: The model (1.3) has an interior equilibrium $P_3 = (x_1, y_1)$ if $s - qE > 0$ and $B < 0$.
- Case $c - mn < 0$: If $\dot{x} = 0$, the model (1.3) has as an isocline

$$y = \frac{rx(x - K)}{aK(m - x)}, \tag{3.4}$$

which is a positive and decreasing function for $m < x < K$, with asymptote at $x = m$.

If $\dot{y} = 0$, the model (1.3) has as isoclines $y = 0$,

$$y = \frac{(s - qE)\left[nx + (c - mn)\right]}{s}, \tag{3.5}$$

and

$$x = -\frac{c - mn}{n}. \tag{3.6}$$

Note that the function (3.5) intercepts with (3.6) at $y = 0$, so the functions (3.4) and (3.5) do not intercept if $s - qE \leq 0$, and implies that the model (1.3) has no interior equilibriums. On the other hand, if $s - qE > 0$, then the functions (3.4) and (3.5) intercept at a single point $P_3 = (x_1, y_1)$. Figure 3 shows the behavior of the isoclines for the case where $c - mn < 0$.

(a) $s - qE < 0$ (b) $s - qE > 0$
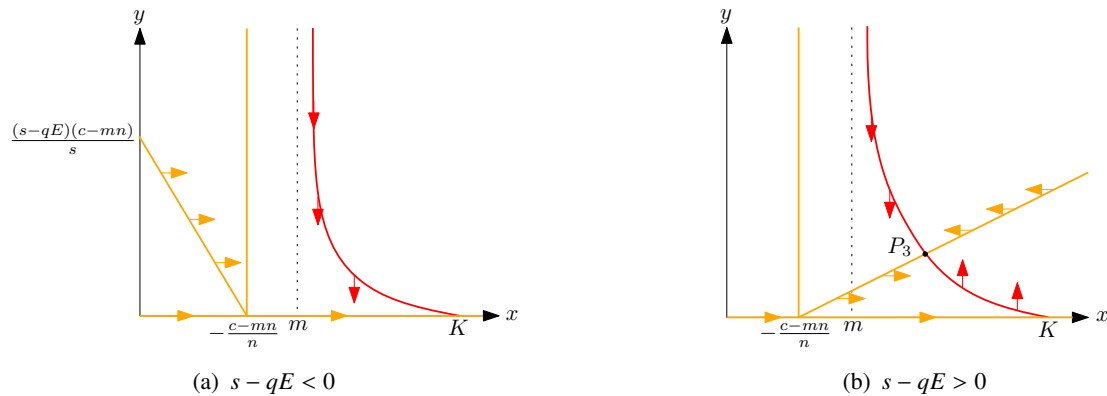
Figure 3. Isoclines of the model (1.3) for the case $c - mn < 0$. Red curve: Isocline $\dot{x} = 0$. Yellow lines: Isoclines $\dot{y} = 0$.

Therefore, the existence of the interior equilibrium $P_3 \in \Omega_m$ is summarized in the following result.

Lemma 3. *If $s - qE \leq 0$, the model (1.3) has no interior equilibrium. If $s - qE > 0$, the model (1.3) has a unique interior equilibrium $P_3 \in \Omega_m$.*

On the other hand, the following result determines the conditions on the local stability of the equilibrium on the model (1.3).

Lemma 4. *Local stability of equilibriums P_1 and P_3 in the model (1.3).*

1) If $s - qE > 0$ then P_1 is a saddle point. If $s - qE < 0$, then P_1 is a locally stable node.

2) If P_3 is an interior equilibrium, then P_3 is locally stable.

Proof. Indeed,

1) As the eigenvalues of the Jacobian matrix $J(x, y)$ of the model (1.3) calculated in P_1,

$$J(P_1) = \begin{bmatrix} -r & -a(m - K) \\ 0 & s - qE \end{bmatrix},$$

are given by $\lambda_1 = -r < 0$ and $\lambda_2 = s - qE$. If $s - qE < 0$ then P_1 is a locally stable node. For $s - qE > 0$, then P_1 is a saddle point.

2) From the Jacobian matrix $J(x, y)$ of the model (1.3) calculated in P_3,

$$J(P_3) = \begin{bmatrix} -\frac{2rx_1 + K(ay_1 - r)}{K} & a(x_1 - m) \\ \frac{nsy_1^2}{(nx_1 + c - mn)^2} & -(s - qE) \end{bmatrix},$$

we have that

$$\text{tr } J(P_3) \quad = \quad -\frac{x_1(A + rs) + B + sK(s - qE)}{sK} > 0,$$

$$\det J(P_3) \quad = \quad \frac{(s - qE)\sqrt{B^2 - 4AC}}{Ks} > 0,$$

where $A > 0$ and $C < 0$ if $c - mn > 0$ and, $A, B, C > 0$ if $c - mn < 0$, with A, B and C as described in (3.2). Let $\triangle_m := \text{tr } J(P_3)^2 - 4\det J(P_3)$. If $\triangle_m < 0$, then P_3 is locally a stable focus. If $\triangle_m > 0$, P_3 is locally a stable node.

Before calculating and determining the global stability of the possible equilibrium points of the model (1.3), the following result shows the non-existence of limit cycles in Ω_m.

Lemma 5. *The model (1.3) has no limit cycles in Ω_m.*

Proof. Let

$$\begin{aligned}
f(x, y) &= rx\left(1 - \frac{x}{K}\right) - a(x - m)y, \\
g(x, y) &= sy\left[1 - \frac{y}{n(x - m) + c}\right] - qEy
\end{aligned} \tag{3.7}$$

and

$$h(x, y) = \frac{K + x}{xy}. \tag{3.8}$$

Since

$$\frac{\partial hf}{\partial x} + \frac{\partial hg}{\partial y} = -\left\{\frac{2rx^3 + aKx^2y + aK^2my}{Kx^2y} + \frac{s(x + K)}{x[n(x - m) + c]}\right\} < 0,$$

for all $(x, y) \in \Omega_m$, that is, for $m \le x$, by the Bendixon - Dilac criterion [31], the model (1.3) has no limit cycles in Ω_m.

Consequently, since the model (1.3) has no limit cycles in Ω_m invariant, as observed in Lemmas 1 and 5, in view of the Poincare - Bendixson Theorem [31] and the local stability of the equilibriums on the model (1.3), shown in Lemma 4, the following result shows conditions for establishing the global stability of the equilibriums P_1 or P_3 in Ω_m.

Theorem 1. *If $s - qE < 0$, then P_1 is a globally asymptotically stable node in Ω_m. If $s - qE > 0$, then P_3 is a globally asymptotically stable equilibrium in Ω_m.*

3.2. Existence of a transcritical bifurcation

The model (1.3) has a transcritical bifurcation when P_3 and P_1 collide, which P_1 transforms from a saddle point to a stable node and P_3 changes from stable to non-existent at Ω_m. The existence of the bifurcation is characterized by the existence of a null eigenvalue in the Jacobian matrix $J(P_1)$, that is, when $s - qE = 0$, shown in the following result.

Theorem 2. *If $s - qE = 0$, then model (1.3) has a transcritical bifurcation around P_1.*

Proof. Let $F(x, y, s)$ and $F_s(x, y, s)$ as the vector field Y and its derivative with respect to s, respectively, that is,

$$F(x, y, s) = \begin{pmatrix} rx\left(1 - \dfrac{x}{K}\right) - a(x - m)y \\ sy\left[1 - \dfrac{y}{n(x - m) + c}\right] - qEy \end{pmatrix}, \quad F_s(x, y, s) = \begin{pmatrix} 0 \\ y\left[1 - \dfrac{y}{n(x - m) + c}\right] \end{pmatrix},$$

and V, W as the eigenvectors associated with the null eigenvalue in the Jacobian matrix $J(P_1)$ and $J(P_1)^T$, that is,

$$V = \begin{pmatrix} \dfrac{a(K - m)}{r} \\ 1 \end{pmatrix}, \quad W = \begin{pmatrix} 0 \\ -1 \end{pmatrix}.$$

If $s = s_0 := qE$, by the transcritical bifurcation Theorem [32], three conditions must be guaranteed:

1) $W^T F_s(P_1, s_0) = 0$: Since $F_s(P_1, s_0) = (0, 0)^T$, the result is guaranteed.

2) $W^T[DF_s(P_1, s_0)V] \neq 0$: Since $DF_s(P_1, s_0)V = (0, -1)^T$, then $W^T[DF_s(P_1, s_0)V] = 1 > 0$.

3) $W^T[D^2F(P_1, s_0)(V, V)] \neq 0$, where $V = (v_1, v_2)^T$: Since

$$D^2F(P_1, s_0)(V, V) \quad = \quad \begin{pmatrix} \dfrac{\partial^2 F_1}{\partial x^2}v_1v_1 + 2\dfrac{\partial^2 F_1}{\partial x \partial y}v_1v_2 + \dfrac{\partial^2 F_1}{\partial y^2}v_2v_2 \\ \dfrac{\partial^2 F_2}{\partial x^2}v_1v_1 + 2\dfrac{\partial^2 F_2}{\partial x \partial y}v_1v_2 + \dfrac{\partial^2 F_2}{\partial y^2}v_2v_2 \end{pmatrix}$$

$$= \quad \begin{pmatrix} \dfrac{2a^2(m - 2K)(K - m)}{Kr} \\ -\dfrac{2}{n(K - m) + c} \end{pmatrix},$$

then $W^T[D^2F(P_1, s_0)(V, V)] = \frac{2}{n(K-m)+c} > 0$.

Therefore, the model (2.1) has a transcritical bifurcation at $s = qE$.

3.3. Bifurcation diagram

We analyze the cases in which the parameters m and E can modify the phase diagrams of the model (1.3) using the results found by the qualitative analysis presented in Subsection 3.1. Indeed, in Figure 4 we observe all possible dynamics of the model (1.3) in Ω_m with respect to the bifurcation curve in the plane (m, E), shown in Figure 4(a).

In this case, and as observed in Figure 4(b)–(d), the phase portraits in Ω_m representing each bifurcation region, shown in Figure 4(a), are given by:

- In region I, the trajectories φ_X, regardless of the initial condition $(x(0), y(0)) \in \Omega_m$, converge to the equilibrium P_1 in Ω_m. Note that $P_3 \notin \Omega_m$ as seen in Figure 4(b).
- In regions II and III, the equilibrium $P_3 \in \Omega_m$ and the trajectories φ_X converge to P_3, where P_3 is a node in region II and a focus in region III. Figure 4(c) and (d) show the dynamics of the model (1.3) in Ω_m for regions II and III, respectively.

(a) Bifurcation curves in the plane (m, E)

(b) Region I

(c) Region II

(d) Region III
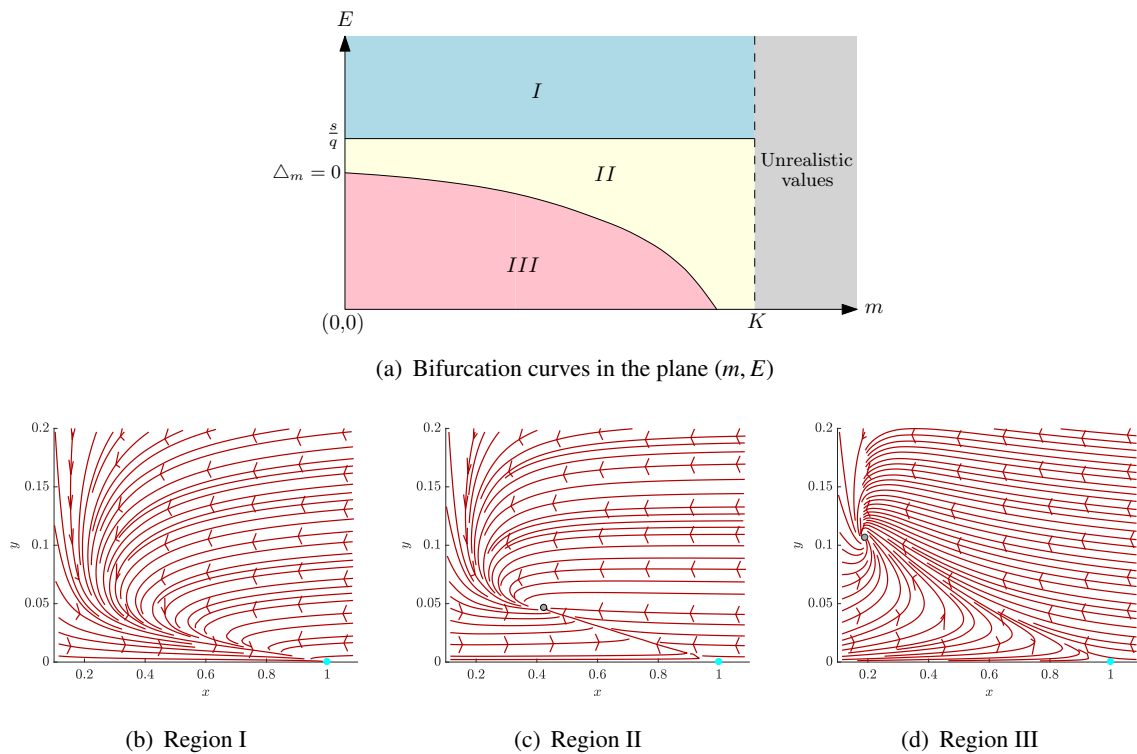
Figure 4. Bifurcation diagram of the model (1.3) in the plane (m, E) and phase portraits in Ω_m characterizing each region, with fixed parameters: $a = 1.5$, $c = 0.1$, $K = q = 1$, $n = 0.7$, $r = 0.09$ and $s = 0.07$. Turquoise point: P_1. Gray point: P_3. Region I: P_1 is a globally asymptotically stable in Ω_m. Region II: P_3 is a globally asymptotically stable node in Ω_m. Region III: P_3 is a globally asymptotically stable focus in Ω_m.

4. Non-constant refuge of prey

If the refuge constant for prey to be consumed by the predator is removed, i.e., when $m = 0$, the dynamics of prey $x(t)$ and predators $y(t)$ is given by the model (1.2) defined in the biological sense region

$$\Omega_0 = \left\{ (x, y) \in \mathbb{R}^2 : 0 \leq x \leq K, 0 \leq y \leq nK + c \right\}.$$

The following result determines that the model (1.2) is mathematically correct and biologically feasible, and that the trajectories φ_W are uniformly bounded, whose proof is equivalent to that shown in Lemmas 1 and 2 and will be omitted for brevity.

Lemma 6. *The model (1.2) has a unique trajectory φ_W, with initial condition $(x(0), y(0)) \in \Omega_m$. Moreover, Ω_0 is invariant and the trajectories φ_W of the model (1.2) are uniformly bounded.*

4.1. Local and global qualitative analysis

Before calculating and determining the local and global stability of the possible equilibrium points of the model (1.2), the following result shows the non-existence of limit cycles in Ω_0.

Lemma 7. *The model (1.2) has no limit cycles in Ω_0.*

Proof. Let

$$
\begin{aligned}
\overline{f}(x,y) &= rx\left(1 - \frac{x}{K}\right) - axy, \\
\overline{g}(x,y) &= sy\left(1 - \frac{y}{nx+c}\right) - qEy
\end{aligned}
\tag{4.1}
$$

and $h(x,y)$ defined in (3.8). Since

$$
\frac{\partial h\overline{f}}{\partial x} + \frac{\partial h\overline{g}}{\partial y} = -\left[\frac{2rx + aKy}{Ky} + \frac{s(x+K)}{nx^2 + cx}\right] < 0,
$$

for all $(x,y) \in \Omega_0$, by the Bendixon-Dilac criterion, the model (1.2) has no limit cycles in Ω_0.

On the other hand, the equilibriums in the model (1.2) on the (x,y) axes are given by: $\overline{P}_0 = (0,0)$, $\overline{P}_1 = (K,0)$ and $\overline{P}_2 = \left(0, \frac{c(s-qE)}{s}\right)$ if $s - qE > 0$. Let

$$
\phi = \frac{rs}{ac(s-qE)},
\tag{4.2}
$$

if $s - qE > 0$ and $1 < \phi$, the model (1.2) has an interior equilibrium $\overline{P}_3 = (\overline{x}, \overline{y}) \in \Omega_0$, with

$$
\overline{x} = \frac{K(\phi - 1)}{aKn(s-qE) + rs} \quad \text{and} \quad \overline{y} = \frac{(s-qE)(n\overline{x}+c)}{s}.
\tag{4.3}
$$

The following result determines the conditions on the local stability of the equilibrium on the model (1.2).

Lemma 8. *Local stability of equilibriums* $\overline{P}_0$, $\overline{P}_1$, $\overline{P}_2$ *and* $\overline{P}_3$ *in the model (1.2).*

1) If $s - qE > 0$, then $\overline{P}_0$ is a locally unstable node. If $s - qE < 0$, then $\overline{P}_0$ is a saddle point.

2) If $s - qE > 0$, then $\overline{P}_1$ is a saddle point. If $s - qE < 0$, then $\overline{P}_1$ is a locally stable node.

3) Let $s - qE > 0$. If $\phi < 1$, then $\overline{P}_2$ is locally a stable node. If $1 < \phi$, then $\overline{P}_2$ is a saddle point.

4) If $\overline{P}_3$ is an interior equilibrium, then $\overline{P}_3$ is locally stable.

Proof. Indeed,

1) From the Jacobian matrix $\overline{J}(x,y)$ of the model (1.2) calculated at $\overline{P}_0$, that is,

$$
\overline{J}(\overline{P}_0) = \begin{bmatrix} r & 0 \\ 0 & s - qE \end{bmatrix},
$$

we have as eigenvalues: $\lambda_1 = r > 0$ and $\lambda_2 = s - qE$. Consequently, if $s - qE > 0$ then $\overline{P}_0$ is a locally unstable node. However, for $s - qE < 0$, then $\overline{P}_0$ is a saddle point.

2) As the eigenvalues of the Jacobian matrix $\overline{J}(x,y)$ of the model (1.2) calculated in $\overline{P}_1$,

$$
\overline{J}(\overline{P}_1) = \begin{bmatrix} -r & -aK \\ 0 & s - qE \end{bmatrix},
$$

are given by $\lambda_1 = -r < 0$ and $\lambda_2 = s - qE$. If $s - qE < 0$ then $\overline{P}_1$ is a locally stable node. If $s - qE > 0$, then $\overline{P}_1$ is a saddle point.

3) From the Jacobian matrix $\overline{J}(x, y)$ of the model (1.2) calculated in $\overline{P}_2$,

$$\overline{J}(\overline{P}_2) = \begin{bmatrix} \frac{\phi-1}{s} & 0 \\ \frac{n(s-qE)^2}{s} & -(s-qE) \end{bmatrix},$$

we have as eigenvalues: $\lambda_1 = \frac{\phi-1}{s}$ and $\lambda_2 = -(s-qE) < 0$. Therefore, if $\phi < 1$, then $\overline{P}_2$ is locally a stable node. If $1 < \phi$, then $\overline{P}_2$ is a saddle point.

4) From the Jacobian matrix $\overline{J}(x, y)$ of the model (1.2) calculated in $\overline{P}_3$,

$$\overline{J}(\overline{P}_3) = \begin{bmatrix} \frac{-2r\overline{x}+(a\overline{y}-r)}{k} & -a\overline{x} \\ \frac{n(s-qE)^2}{s} & -(s-qE) \end{bmatrix},$$

we have that

$$\operatorname{tr} \overline{J}(\overline{P}_3) = \frac{r(1-\phi) - [anK(s-qE) + rs](s-qE)}{rs + anK(s-qE)} < 0,$$

$$\det \overline{J}(\overline{P}_3) = \frac{(s-qE)(\phi-1)}{s} > 0.$$

Therefore, $\overline{P}_3$ is locally stable. Let $\overline{\triangle} := \operatorname{tr} \overline{J}(\overline{P}_3)^2 - 4\det \overline{J}(\overline{P}_3)$. If $\overline{\triangle} < 0$, then $\overline{P}_3$ is locally a stable focus. If $\overline{\triangle} > 0$, $\overline{P}_3$ is locally a stable node.

Consequently, and equivalently to what is shown by Theorem 1, the following result shows conditions for establishing the global stability of the equilibriums $\overline{P}_1$, $\overline{P}_2$ or $\overline{P}_3$.

Theorem 3. *If $s - qE < 0$, then $\overline{P}_1$ is a globally asymptotically stable node. If $s - qE > 0$ and $\phi < 1$ then $\overline{P}_2$ is a globally asymptotically stable node. If $s - qE > 0$ and $1 < \phi$, then $\overline{P}_3$ is a globally asymptotically stable equilibrium.*

In particular, model (1.2) has two transcritical bifurcations as observed in the following result, whose proof is analogous to Theorem 2.
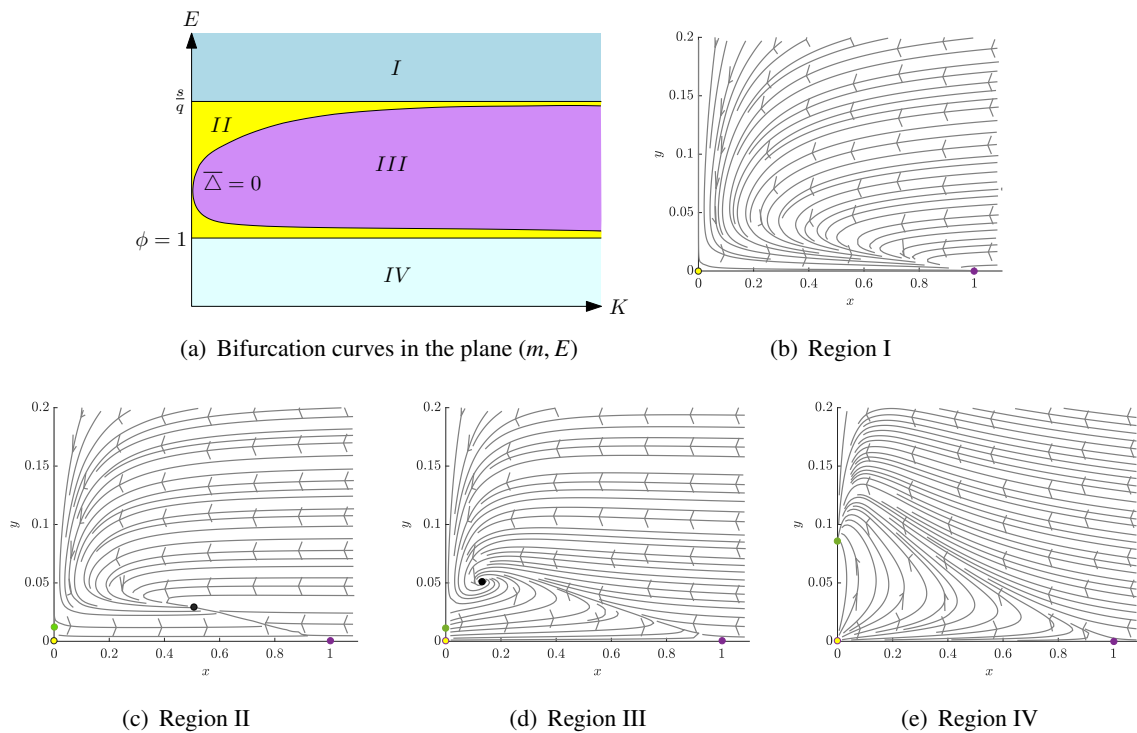
Theorem 4. *Existence of transcritical bifurcation in the model (1.2).*

1) If $s - qE = 0$, the model has a bifurcation around $\overline{P}_1$.

2) If $\phi = 1$ and $s - qE > 0$, the model has a bifurcation around $\overline{P}_2$.

4.2. Bifurcation diagram

We analyze the cases in which the parameters K and E can alter the behaviors in the trajectories of the model (1.2). Indeed, Figure 5 we observe all possible dynamics of the model (1.2) with respect to the bifurcation curve in the plane (K, E), shown in Figure 5(a), whose phase portraits representing each bifurcation region are described as follows:

- In region I, as observed in Figure 5(b), $\overline{P}_{2,3} \notin \Omega_0$ and the trajectories φ_W, regardless of the initial condition $(x(0), y(0)) \in \Omega_0$, converge to the equilibrium $\overline{P}_1 \in \Omega_0$.
- In regions II and III, the equilibriums $\overline{P}_{2,3} \in \Omega_0$ but φ_W converges to $\overline{P}_3$, where $\overline{P}_3$ is a node in region II and a focus in region III as observed in Figure 5(c) and (d), respectively.
- In region IV, $\overline{P}_3 \notin \Omega_0$ and φ_W converges to $\overline{P}_2$ as seen in Figure 5(e).

(a) Bifurcation curves in the plane (m, E)

(b) Region I

(c) Region II

(d) Region III

(e) Region IV

Figure 5. Bifurcation diagram of the model (1.3) in the plane (m, E) and phase portraits characterizing each region, with fixed parameters: $a = 1.5$, $c = 0.1$, $K = q = 1$, $n = 0.7$, $r = 0.09$ and $s = 0.07$. Yellow point: $\overline{P}_0$. Purple point: $\overline{P}_1$. Green point: $\overline{P}_2$. Black point: $\overline{P}_3$. Region I: $\overline{P}_1$ is a globally asymptotically stable in Ω_0 and $\overline{P}_{2,3} \notin \Omega_0$. Region II: $\overline{P}_3$ is a globally asymptotically stable node in Ω_0. Region III: $\overline{P}_3$ is a globally asymptotically stable focus in Ω_0. Region IV: $\overline{P}_3 \notin \Omega_0$ and $\overline{P}_2$ is a globally asymptotically stable node.

5. Non-predatory model

In contrast to the assumptions made for the formulation of the model (1.3) with $x(0) < m$, if the prey $x(t)$ are protected at all times from being consumed by the predator, the dynamics between the two species is given by the model (1.4) defined in the biological sense region

$$\tilde{\Omega} = \left\{ (x, y) \in \mathbb{R}^2 : 0 \leq x \leq K, 0 \leq y \leq c \right\}.$$

The following result, without proof, shows the non-existence of limit cycles in the model (1.4), so there are no periodic trajectories in the dynamics of $x(t)$ and $y(t)$.

Lemma 9. *In the model (1.4) there are no limit cycles on $\tilde{\Omega}$.*

On the other hand, the model (1.4) has as equilibriums $\tilde{P}_0 = (0, 0)$ and $\tilde{P}_1 = (K, 0)$. However, if $s - qE > 0$, the model (1.4) has two additional equilibrium given by $\tilde{P}_2 = \left(0, \frac{c(s-qE)}{s} \right)$ and $\tilde{P}_3 = \left(K, \frac{c(s-qE)}{s} \right)$. Local and global stability of each equilibrium point are shown in the following results, whose phase portraits are observed in Figure 6.

(a) $s - qE < 0$ (b) $s - qE > 0$
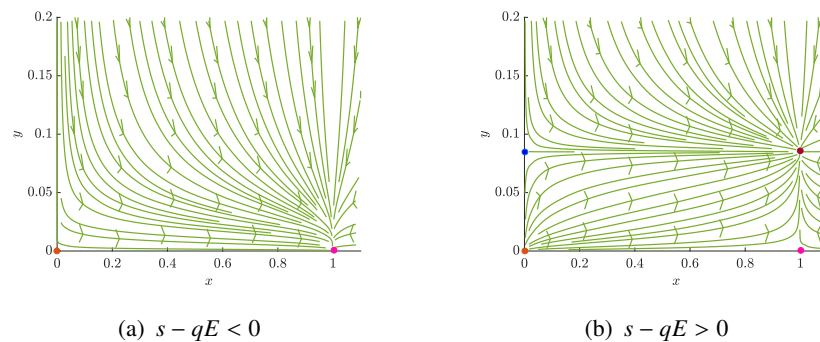
Figure 6. Phase portraits in the model (1.4) with fixed parameters: $K = q = 1$, $c = 0.2$, $r = 0.09$ and $s = 0.07$. Orange point: $\tilde{P}_0$. Pink point: $\tilde{P}_1$. Blue point: $\tilde{P}_2$. Dark red point: $\tilde{P}_3$. If $s - qE < 0$, $\varphi_Y \to \tilde{P}_1$ when $t \to \infty$. If $s - qE > 0$, $\varphi_Y \to \tilde{P}_3$ when $t \to \infty$.

Lemma 10. *If $s - qE < 0$, that is, if $\tilde{P}_{2,3} \notin \tilde{\Omega}$, the equilibrium $\tilde{P}_0$ is locally a saddle point and $\tilde{P}_1$ is locally a stable node. If $s - qE > 0$ we have that $\tilde{P}_{1,2}$ are locally a saddle point, $\tilde{P}_3$ and $\tilde{P}_0$ are locally a stable and unstable node, respectively.*

Theorem 5. *If $s - qE > 0$, then $\tilde{P}_3$ in the model (1.4) is globally asymptotically stable. If $s - qE < 0$ then $\tilde{P}_1$ is globally asymptotically stable.*

6. Protection of prey subject to the threshold value

From the hypotheses proposed to relate the growth and interaction of prey and predators given in Sections 3–5, if a constant quantity of prey $m > 0$ take refuge, which avoids being consumed by the predator, when its population size is lower than its critical value $M > 0$, where $0 < m < M < K$, and does not maintain contact with the predator if $x < m$, the final dynamics between prey and predators is described by the discontinuous model (1.6), equivalent to:

$$V(x,y) = \begin{cases} W(x,y) = \begin{pmatrix} rx\left(1 - \dfrac{x}{K}\right) - axy \\ sy\left(1 - \dfrac{y}{nx + c}\right) - qEy \end{pmatrix}, & x > M \\[3em] X(x,y) = \begin{pmatrix} rx\left(1 - \dfrac{x}{K}\right) - a(x-m)y \\ sy\left[1 - \dfrac{y}{n(x-m) + c}\right] - qEy \end{pmatrix}, & m < x < M \\[3em] Y(x,y) = \begin{pmatrix} rx\left(1 - \dfrac{x}{K}\right) \\ sy\left(1 - \dfrac{y}{c}\right) - qEy \end{pmatrix}, & x < m \end{cases} \tag{6.1}$$

where

$$\begin{aligned} \Sigma^+ &= \left\{(x,y) \in \mathbb{R}^2 : M < x \le K, 0 \le y \le nK + c\right\}, \\ \Sigma_1 &= \{(M,y) \in \mathbb{R}^2 : 0 \le y \le nK + c\}, \\ \Sigma^* &= \{(x,y) \in \mathbb{R}^2 : m < x < M, 0 \le y \le nK + c\}, \\ \Sigma_2 &= \{(m,y) \in \mathbb{R}^2 : 0 \le y \le nK + c\}, \\ \Sigma^- &= \{(x,y) \in \mathbb{R}^2 : 0 \le x < m, 0 \le y \le nK + c\}. \end{aligned}$$

To perform a qualitative analysis of the discontinuous model (6.1) we must calculate the equilibrium points, the regions $\Sigma_{1,2}^{s,e,c}$ that divide $\Sigma_{1,2}$ and, the sliding segment $Z_{1,2}^s$ in $\Sigma_{1,2}$.

6.1. Local stability of equilibrium points

From the equilibrium in the vector fields W, X, Y, as observed in Section 4, 3 and 5 respectively, we have that the equilibriums of the discontinuous model (6.1) on the coordinate axes (x, y) are given by: $\tilde{P}_0 = (0, 0) \in \Sigma^-$, $\tilde{P}_2 = \left(0, \frac{c(s-qE)}{s}\right) \in \Sigma^-$ if $s - qE > 0$ and, $\overline{P}_1 = (0, K) \in \Sigma^+$.

Moreover, if $s - qE > 0$ and $m < x_1 < M$, the discontinuous model (6.1) has an interior equilibrium given by $P_3 = (x_1, y_1) \in \Sigma^*$, with x_1 and y_1 as described in (3.3) and (3.1), respectively. Also, if $1 < \phi$ and $M < \overline{x}$, the discontinuous model (6.1) has another interior equilibrium given by $\overline{P}_3 = (\overline{x}, \overline{y}) \in \Sigma^+$, with $\overline{x}$ and $\overline{y}$ as described in (4.3). The local stability of each equilibrium is shown in the Lemmas 4, 8 and 10.

However, the interior equilibriums P_3 and $\overline{P}_3$ do not coexist in the discontinuous model (6.1), as shown in the following result.

Lemma 11. *If $s - qE > 0$ and $1 < \phi$, then P_3 and $\overline{P}_3$ do not coexist in the discontinuous model (6.1).*

Proof. Since $ac(s - qE) > a(c - 2m)(s - qE)$, if $1 < \phi$ then $ac(s - qE) > rs > a(c - 2m)(s - qE)$ or $ac(s - qE) > a(c - 2m)(s - qE) > rs$. In either case, $\overline{x} < x_1$. Therefore, if $M < \overline{x}$ then $\overline{P}_3 \in \Sigma^+$ and $P_3 \notin \Sigma^*$. If $\overline{x} < M < x_1$, then $\overline{P}_3 \notin \Sigma^+$ and $P_3 \notin \Sigma^*$. If $x_1 < M$ then $\overline{P}_3 \notin \Sigma^+$ and $P_3 \in \Sigma^*$. $\qquad\square$

6.2. Existence of pseudo-equilibrium and tangent points in Σ_1

If $f_1(x, y) = x - M$, then for all $p \in \Sigma_1$,

$$
\begin{aligned}
Wf_1(p) &= \langle W(p), \mathrm{grad} f_1(p) \rangle &= rM\left(1 - \frac{M}{K}\right) - aMy, \\
Xf_1(p) &= \langle X(p), \mathrm{grad} f_1(p) \rangle &= rM\left(1 - \frac{M}{K}\right) - a(M - m)y.
\end{aligned}
$$

Since $\frac{r(K-M)}{aK} < \frac{rM(K-M)}{aK(M-m)}$, then

$$
\begin{aligned}
\Sigma_1^s &= \left\{(M, y) \in \mathbb{R}^2 : \frac{r(K-M)}{aK} < y < \frac{rM(K-M)}{aK(M-m)}\right\}, \\
\Sigma_1^c &= \left\{(M, y) \in \mathbb{R}^2 : 0 < y < \frac{r(K-M)}{aK} \text{ or } \frac{rP(K-M)}{aK(M-m)} < y < n(K-m) + c\right\}, \\
\Sigma_1^e &= \emptyset.
\end{aligned}
$$

In addition, the sliding segment Σ_1^s has two tangent points given by:

$$
\overline{T} = \left(M, \frac{r(K-M)}{aK}\right) \quad \text{and} \quad T = \left(M, \frac{rM(K-M)}{aK(M-m)}\right),
$$

where the tangent point $\overline{T}$ is visible if $W^2 f(\overline{T}) = \left\langle W(\overline{T}), \mathrm{grad} W f_1(\overline{T}) \right\rangle > 0$, that is,

$$
rs(K - M) > aK(nM + c)(s - qE),
$$

and invisible if

$$
rs(K - M) < aK(nM + c)(s - qE).
$$

Similarly, the tangent point T is visible if $X^2 f_1(T) = \langle X(T), \mathrm{grad} X f_1(T) \rangle < 0$, that is,

$$rsM(K - M) < aK[c + n(M - m)](M - m)(s - qE)$$

and invisible if

$$rsM(K - M) > aK[c + n(M - m)](M - m)(s - qE).$$

The following result summarizes the behavior of the tangent points on the model, whose proof will be omitted.

Lemma 12. *Let T and $\overline{T}$ tangent points of the discontinuous model (6.1), with ϕ as described in (4.2).*

1) If $s - qE < 0$ then $\overline{T}$ is visible and T is invisible to all $m < M < K$.

2) For $s - qE > 0$,

(a) If $\phi < 1$, $\overline{T}$ is invisible to all $m < M < K$. If $1 < \phi$, $\overline{T}$ is invisible if $\overline{P}_3 \notin \Sigma^+$, and visible if $\overline{P}_3 \in \Sigma^+$.

(b) The tangent point T is visible if $P_3 \in \Sigma^*$, and invisible if $P_3 \notin \Sigma^*$.

On the other hand, the vector field of the sliding segment $Z_1^s(p) = (Z_{1x}^s, Z_{1y}^s)^T$, with $p \in \Sigma_1^s$, is given by

$$Z_1^s(p) = \left(\begin{array}{c} 0 \\ \dfrac{y\{aK(nM + c)[n(M - m) + c](s - qE) - asKy[n(2M - m) + c] + nrsM(K - M)\}}{aK(nM + c)[n(M - m) + c]} \end{array} \right),$$

with pseudo-equilibrium $PN = (M, y_p) \in \Sigma_1^s$, where

$$y_p = \frac{aK(nM + c)[n(M - m) + c](s - qE) + nrsM(K - M)}{asK[n(2M - m) + c]},$$

which corresponds to a stable pseudo-node because $Z_{1y}^s > 0$ if $y < y_p$ and $Z_{1y}^s < 0$ if $y > y_p$.

The following result shows conditions for the existence of the stable pseudo-node PN.

Lemma 13. *Conditions for the existence of the stable pseudo-node PN in the discontinuous model (6.1), with ϕ as described in (4.2).*

1) If $s - qE < 0$ then $PN \notin \Sigma_1^s$.

2) For $s - qE > 0$,

(a) If $\phi < 1$, then $PN \in \Sigma_1^s$ if, and only if, $P_3 \notin \Sigma^*$.

(b) If $1 < \phi$, the pseudo-nodo $PN \in \Sigma_1^s$ if, and only if, $P_3 \notin \Sigma^*$ and $\overline{P}_3 \notin \Sigma^+$.

Proof. Note that $PN \in \Sigma_1^s$ if, and only if, $\frac{r(K-M)}{aK} < y_p < \frac{rM(K-M)}{aK(M-m)}$, that is, $rs(K-M) < aK(nM+c)(s-qE)$ and $rsM(K - M) > aK[n(M - m) + c](M - m)(s - qE)$. In this case, if $s - qE < 0$, then $PN \notin \Sigma_1^s$. However, if $s - qE > 0$, $PN \in \Sigma_1^s$ if, and only if,

$$\frac{K[\phi - 1]}{anK(s - qE) + rs} < M, \tag{6.2}$$

and

$$M < \frac{-B + \sqrt{B^2 - 4AC}}{2A}, \tag{6.3}$$

with A, B and C as described in (3.2).

Therefore, if $\phi < 1$ then (6.2) is obtained for all $M > 0$ and (6.3) is satisfied if, and only if, $\overline{P}_3 \notin \Sigma^+$. However, if $1 < \phi$, then $PN \in \Sigma_1^s$ if, and only if, $\overline{x} < M < x_1$, that is, $P_3 \notin \Sigma^*$ and $\overline{P}_3 \notin \Sigma^+$.

In summary, and in view of the results shown in Lemmas 12 and 13 it follows that if $\overline{P}_3 \in \Sigma^+$, then $\overline{T}$ is visible, T is invisible and $\Sigma_1^s = \overrightarrow{\overline{T}T}$. On the other hand, if $P_3 \in \Sigma^*$, then $\overline{T}$ is invisible, T is visible and $\Sigma_1^s = \overleftarrow{\overline{T}T}$. Conversely, if $PN \in \Sigma_1^s$, then T and $\overline{T}$ are invisible and $\Sigma_1^s = \overrightarrow{TPN}\overleftarrow{PN\overline{T}}$.

6.3. Non-existence of pseudo-equilibrium and tangent points in Σ_2

In this case, if $f_2(x, y) = x - m$, then for all $p \in \Sigma_2$,

$$Xf_2(p) = Yf_2(p) = rm\left(1 - \frac{m}{K}\right) > 0,$$

and $\Sigma_2 = \Sigma_2^c$, that is, the trajectories φ_V with initial condition $(x(0), y(0)) \in \Sigma^-$ must cross Σ_2 and reach Σ^*, so there are no pseudo-equilibriums and tangent points in Σ_2.

### 6.4. Global stability of equilibrium and pseudo-equilibrium

It is important to determine the global stability of the equilibriums $\overline{P}_1$, P_3, $\overline{P}_3$ and of the pseudo-equilibrium PN. Indeed, for the case where the pseudo-equilibrium $PN \in \Sigma_1^s$, the trajectories φ_V of the discontinuous model (6.1) converge to PN for all $(x(0), y(0)) \in \Sigma^- \cup \Sigma_2 \cup \Sigma^* \cup \Sigma_1 \cup \Sigma^+$, and thus PN is globally asymptotically stable, as observed in the following result, whose proof was inspired by [28, 33, 34].

Theorem 6. *If $PN \in \Sigma^s$, then PN is globally asymptotically stable.*

Proof. Since $PN \in \Sigma_1^s$ is locally stable, $\tilde{P}_0 \in \Sigma^-$ is unstable, $P_1 \in \Sigma^+$ and $\tilde{P}_2 \in \Sigma^-$ are saddle points, $P_3 \notin \Sigma^*$ and $\overline{P}_3 \notin \Sigma^+$, to guarantee the global asymptotic stability of PN five conditions must be proved:

1) *There are no limit cycles in Σ^+, Σ^* and Σ^-:* By the Lemmas 7, 5 and 9 the non-existence of limit cycles in Σ^+, Σ^* and Σ^-, respectively, is guaranteed.

2) *There is no periodic trajectory for discontinuous model (6.1) which contains a part of Σ_1^s:* Since the pseudo-equilibrium $PN \in \Sigma_1^s$ is stable, there is not closed orbit for discontinuous model (6.1) containing a part of Σ_1^s.

3) *There is no periodic trajectory which contains Σ^- and Σ^*:* Since $\Sigma_2 = \Sigma_2^c$ and from the dynamics of the vector field Y, formed by systems of autonomous and independent differential equations, no closed trajectory can be formed by unions of trajectories in Σ^* and Σ^-.

4) *There is no periodic trajectory which contains Σ^-, Σ^*, Σ_1^s and Σ^+ :* Analogous to the previous reasoning.

5) *There is no closed trajectory which contains Σ^*, Σ_1^s and Σ^+:* Indeed, if it is assumed that there is a closed trajectory Γ of discontinuous model (6.1), which passes through Σ_1 and encloses Σ_1^s, let Q and N as the intersection points of Γ and Σ_1, respectively, as observed in Figure 7. Similarly, let $Q_1 = Q + a_1(\theta)$ and $N_1 = N - a_2(\theta)$, with intersection points of Γ and the line $x = M - \theta$, respectively, and $Q_2 = Q + b_1(\theta)$ and $N_2 = N - b_2(\theta)$ as the intersection points of Γ and $x = Q + \theta$, where $\theta > 0$ is sufficiently small. Moreover, $a_{1,2}(\theta)$ and $b_{1,2}(\theta)$ are continuous with respect θ and $a_{1,2}(\theta), b_{1,2}(\theta) \to 0$ when $\theta \to 0$.
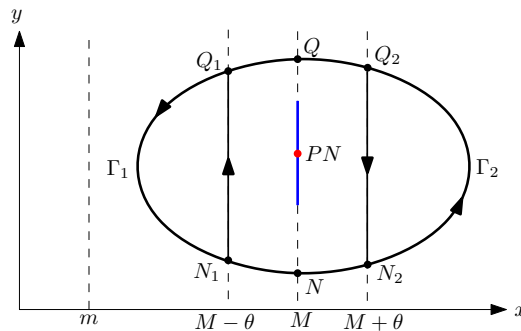
Figure 7. Limit cycle Γ of discontinuous model (6.1).

As shown in Figure 7, the Γ_1 and $\overrightarrow{N_1 Q_1}$ is locate in the region Σ^*. Similarly, the Γ_2 and $\overrightarrow{Q_2 N_2}$ is locate in the region Σ^+. Furthermore, the dynamics of discontinuous model (6.1) in region Σ^+ is represented by (4.1) If $\partial \Sigma^+$ denote the boundary of Σ^+, by using Green's Theorem [31], with $h(x, y)$ as in (3.8), we have

$$
\begin{aligned}
\iint_{\Sigma^+} \left(\frac{\partial h \overline{f}}{\partial x} + \frac{\partial h \overline{g}}{\partial y} \right) d\sigma &= \iint_{\Sigma^+} \frac{\partial h \overline{f}}{\partial x} d\sigma + \iint_{\Sigma^+} \frac{\partial h \overline{g}}{\partial y} d\sigma \\
&= \oint_{\partial \Sigma^+} h \overline{f} dy - \oint_{\partial \Sigma^+} h \overline{g} dx \\
&= \left(\int_{\Gamma_2} h \overline{f} dy + \int_{\overrightarrow{Q_2 N_2}} h \overline{f} dy \right) \\
&\quad - \left(\int_{\Gamma_2} h \overline{g} dx + \int_{\overrightarrow{Q_2 N_2}} h \overline{g} dx \right) \\
&= \int_{\overrightarrow{Q_2 N_2}} h \overline{f} dy,
\end{aligned}
\tag{6.4}
$$

where $dx = \overline{f}(x, y)dt$, $dy = \overline{g}(x, y)dt$, and there is no change of x in $\overrightarrow{Q_2 N_2}$, then

$$
\int_{\overrightarrow{Q_2 N_2}} h \overline{g} dx = \int_{M+\theta}^{M+\theta} h \overline{g} dx = 0.
$$

Similarly, if the dynamics in Σ^* is represented by (3.7), by Green's Theorem,

$$
\iint_{\Sigma^*} \left(\frac{\partial h f}{\partial x} + \frac{\partial h g}{\partial y} \right) d\sigma = \int_{\overrightarrow{N_1 Q_1}} h f dy.
\tag{6.5}
$$

Suppose that $\Sigma_{10}^* \subset \Sigma^*$ and

$$\epsilon = \iint_{\Sigma_{10}^*} \left(\frac{\partial hf}{\partial x} + \frac{\partial hg}{\partial y} \right) \mathrm{d}\sigma = \oint_{\partial\Sigma_{10}^*} (hf\mathrm{d}y - hg\mathrm{d}y) > 0. \tag{6.6}$$

From Lemma 5, and based in (6.6), we have

$$0 < \epsilon < \int_{\overrightarrow{Q_2 N_2}} h\overline{f}\mathrm{d}y + \int_{\overrightarrow{N_1 Q_1}} hf\mathrm{d}y. \tag{6.7}$$

As observed in Figure 7, if $\theta \to 0$ in the sum of (6.4) and (6.5) we have that

$$
\begin{aligned}
\lim_{\theta \to 0} \left(\int_{\overrightarrow{Q_2 N_2}} h\overline{f}\mathrm{d}y + \int_{\overrightarrow{N_1 Q_1}} hf\mathrm{d}y \right) &= \lim_{\theta \to 0} \int_{N-b_2(\theta)}^{Q+b_1(\theta)} \left\{ \frac{k+M}{My} \left[rM\left(1 - \frac{M}{K}\right) - aMy \right] \right\} \mathrm{d}y \\
&\quad - \lim_{\theta \to 0} \int_{N-a_2(\theta)}^{Q+a_1(\theta)} \left\{ \frac{k+M}{My} \left[rM\left(1 - \frac{M}{K}\right) - a(M-m)y \right] \right\} \mathrm{d}y \\
&= \frac{am(K+M)}{M}(N-Q) < 0.
\end{aligned}
\tag{6.8}
$$

Then (6.7) holds, which contradicts to (6.8). Thus there is no closed trajectory containing Σ_1^s and PN. Therefore, PN is globally asymptotically stable.

Similarly, if $\overline{P}_3 \in \Sigma^+$, by Theorem 3 and Lemmas 11 and 13, it follows that the trajectories φ_V of the Filippov system (6.1) converge to $\overline{P}_3$ for all $(x(0), y(0)) \in \Sigma^- \cup \Sigma_2 \cup \Sigma^* \cup \Sigma_1 \cup \Sigma^+$. Therefore, the following result shows that the equilibrium $\overline{P}_3$ is globally asymptotically stable, whose proof was inspired by [28, 33, 34].

Theorem 7. *If $\overline{P}_3 \in \Sigma^+$, then $\overline{P}_3$ is globally asymptotically stable.*

Proof. Since $PN \notin \Sigma^s$, $\tilde{P}_0$ is unstable, $\overline{P}_1$ and $\tilde{P}_2$ are saddle points and $P_3 \notin \Sigma^*$, to determine that $\overline{P}_3$ is globally asymptotically stable five conditions must be proved:

1) *There are no limit cycles in Σ^+, Σ^* and Σ^-*: By the Lemmas 7, 5 and 9 we guarantee the non-existence of limit cycles in Σ^+, Σ^* and Σ^-, respectively.

2) *There is no closed trajectory for discontinuous model (6.1) which contains a part of Σ_1^s*: Since $\Sigma_2 = \Sigma_2^c$, $\overline{T}$ is visible and T is invisible, any trajectory φ_V, with initial condition $(x(0), y(0)) \in \Sigma_1^s$, slides over Σ_2^s to $\overline{T}$ and escapes Σ^+, therefore, we will prove that the trajectory φ_V of discontinuous model (6.1) starting from the tangent point $\overline{T}$ cannot enter the Σ_1^s again. Indeed, if the trajectory φ_V starting at $\overline{T}$, encircles $\overline{P}_3$ and intercepts with $\overline{T}$ forming a periodical trajectory Γ, then any φ_V with initial condition outside Γ will not be able to cross Γ, and certainly cannot converge to the equilibrium $\overline{P}_3$, which contradicts the stability of $\overline{P}_3$. Similarly, if the φ_V starting at $\overline{T}$ and encircling the equilibrium $\overline{P}_3$, intercepts Σ_1^s at some point other than $\overline{T}$, then $\overline{P}_3$ must be unstable, which also contradicts to the statement that $\overline{P}_3$ is a stable equilibrium. Therefore, there is no closed trajectory of discontinuous model (6.1) containing part of Σ_1^s.

3) *There is no periodic trajectory which contains Σ^- and Σ^**: Analogous to that shown by the Theorem 6.

4) *There is no periodic trajectory which contains Σ^-, Σ^*, Σ_1^s and Σ^+* : Analogous to that shown by the Theorem 6.

5) *There is no closed trajectory which contains Σ^*, Σ_1^s and Σ^+*: This step is similar to that of Theorem 6, and we omit it here for brevity.

If $s - qE < 0$ and $\phi < 1$, that is, if $P_3 \notin \Sigma^*$ and $\overline{P}_3 \notin \Sigma^+$, by Theorem 1 and Lemmas 12 and 13, the trajectories φ_V of the discontinuous model (6.1) converge to $\overline{P}_1 \in \Sigma^+$ as shown in the following result.

Theorem 8. *If $s - qE < 0$, then $\overline{P}_1 \in \Sigma^+$ is globally asymptotically stable.*

Proof. A similar procedure to that of Theorem 7 can be used to prove this theorem, and we omit it here for brevity.

6.5. Bifurcation diagram

Finally, we analyze the cases in which the parameters M and E can modify the phase diagrams of the discontinuous model (6.1) using the results found by the qualitative analysis presented in Subsection 6.1. Indeed, in Figure 8(b)–(g) show the changes in their phase portraits of the discontinuous model (6.1) with respect to the bifurcation curves in the plane (M, E), represented in Figure 8(a), described as follows:

- In region I, $\overline{P}_1 \in \Sigma^+$ is globally asymptotically stable, this is, φ_V converge to $\overline{P}_1$, regardless of the initial condition $(x(0), y(0)) \in \Sigma^- \cup \Sigma_2 \cup \Sigma^* \cup \Sigma_1 \cup \Sigma^+$, as observed in Figure 8(b).
- In regions II and III, represented in Figure 8(c) and (d) respectively, shows that φ_V converge to $\overline{P}_3 \in \Sigma^+$, where $\overline{P}_3$ is node in region II and a focus in region III.
- In region IV, shown in Figure 8(e), we have that $\varphi_V \to PN \in \Sigma_1^s$ when $t \to \infty$.
- In regions V and VI, represented in Figure 8(f) and (g) respectively, shows that $P_3 \in \Sigma^*$ is a globally asymptotically stable equilibrium, which is a node in region V and a focus in region VI.

7. Conclusions

Since many researchers assume the existence of prey that completely hide from the predator when their population size is below a critical threshold, the proposed discontinuous predator-prey models focus on completely deactivating the predator functional response, which is generally assumed to be nonlinear to enrich the qualitative analysis of the model, if the population size of prey is below the critical threshold [25–29]. However, it could be the case that a constant population size of prey does not manage to hide from the predator, because, for example, they escape from the prey group unnoticed to explore the environment, so the predator functional response should not be deactivated, but modified in such a way that it considers the interaction between the population size of the predator and the unrefuged quantity of prey, where the predator functional response should not necessarily be considered as nonlinear [8, 30].
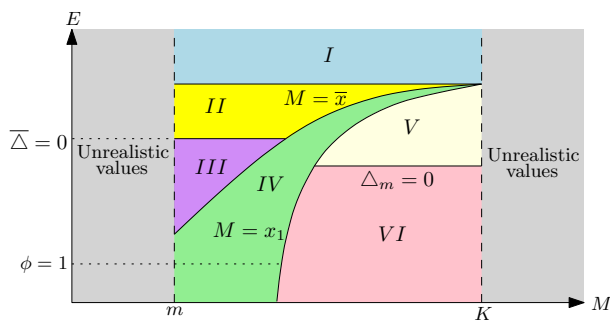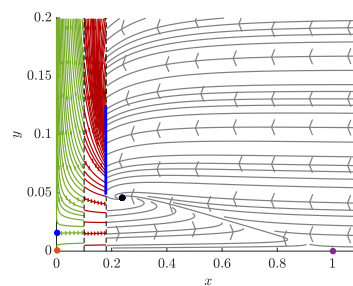
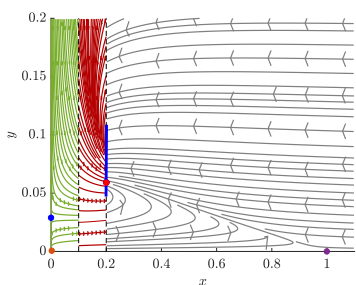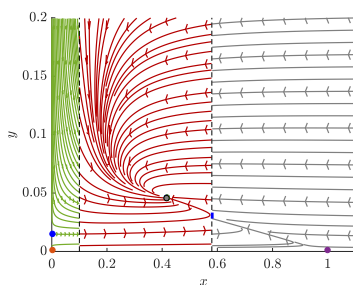(a) Bifurcation curves in the plane (M, E)
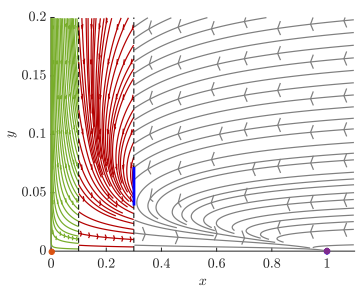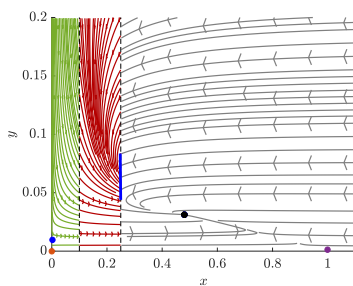
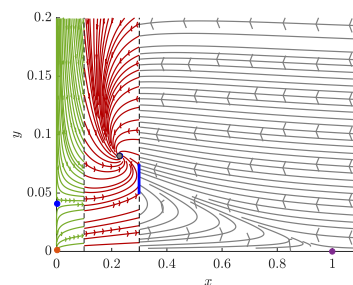
(b) Region I

(c) Region II

(d) Region III

(e) Region IV

(f) Region V

(g) Region VI

Figure 8. Bifurcation diagram of the discontinuous model (6.1) in the plane (E, P) and phase portraits characterizing each region, with fixed parameters: $a = K = q = 1$, $c = 0.2$, $m = 0.1$, $n = 0.7$, $r = 0.09$ and $s = 0.07$. Green vector field: Y. Red vector field: X. Gray vector field: W. Orange point: $\tilde{P}_0$. Purple point: $\overline{P}_1$. Blue point: $\tilde{P}_2$. Black point: $\overline{P}_3$. Gray point: P_3. Red point: PN. Blue line: Σ_2^s. Region I: $\overline{P}_1$ is a globally asymptotically stable and $\tilde{P}_2 \notin \Sigma^-$. Region II: $\overline{P}_3$ is a globally asymptotically stable node. Region III: $\overline{P}_3$ is a globally asymptotically stable focus. Region IV: PN is a globally asymptotically stable node. Region V: P_3 is a globally asymptotically stable node. Region VI: P_3 is a globally asymptotically stable focus.

Therefore, in this work a mathematical model was proposed, by means of a system of discontinuous differential equations, which represents the scientifically observable behavior between a pair of species, prey and predator. From the qualitative analysis of the models (1.2), (1.3) and (1.4), it is determined that the general behavior of the species described in the discontinuous model (1.6) remain in equilibrium over time and no extinction of any species occurs.

Regarding the qualitative analysis of model (1.2), the extinction of predators is determined when the intrinsic birth rate is less than or equal to the product between the harvest coefficient and the capture effort, that is $s - qE < 0$. If this condition among its parameters is not met, the predator species does not become extinct and converges to an equilibrium. However, if the model (1.2) has no internal equilibrium for $s - qE > 0$, the prey should become extinct over time. Moreover, the model (1.2) has two transcritical bifurcations, characterized by the collision of the interior equilibrium with respect to one of its equilibriums located on the coordinate axes, and subsequently, it causes a change in the stability of the equilibrium on the coordinate axis and the disappearance of the interior equilibrium in Ω_0.

On the other hand, and with respect to the qualitative analysis of the model (1.3), this model makes biological sense if the initial population size of prey is greater than or equal to the quantity of refugia, i.e., $m \leq x(0)$. However, for the hypothetical case where $x(0) < m$, the initial condition in the model (1.3) is not constrained if $c - mn \leq 0$, otherwise, if the initial population size of prey is less than $-\frac{(c-mn)}{n}$, the population size of predators grows exponentially, which is biologically absurd. To mitigate this problem, if the initial prey population size is less than $m > 0$, the interaction between prey and predators ceases, and both species attain carrying capacity by logistic growth (1.4), with harvesting for predators, and in that case, the model (1.3) should be applicable when the growth of prey, without interaction with the predator, exceeds the constant refuge of prey.

Unlike the cases of bifurcations in the model (1.2), the model (1.3) has a transcritical bifurcation, associated by the collision, and subsequent change of stability, of the interior equilibrium and the only equilibrium located on the x-axis. The non-existence of the equilibrium on the y-axis in the model (1.3) is associated with the parameter of constant prey refuge $m > 0$, which guarantees the non-extinction of prey. However, the predators described in the model (1.3) could become extinct if the condition of the parameters associated with the model (1.2) are satisfied. In addition, the bifurcation cases for the models (1.2) and (1.3) disagree on an additional bifurcation region in the model (1.2), characterized by prey extinction, that is $s - qE > 0$ and $\phi < 1$, since $m > 0$ prey refuge is not considered in the model (1.3). However, in both models, the predator may become extinct over time if $s - qE \leq 0$.

On the other hand, the transcritical bifurcation in the model (1.3) is transferred to the cases of bifurcations in the discontinuous model (1.6), so the predators, in the same way as in models (1.2) and (1.3), could become extinct if $s - qE \leq 0$, but the value of $m > 0$ guarantees the non-extinction of prey in the discontinuous model (1.6), unlike the model (1.2) in which prey can become extinct over time if $s - qE > 0$ and $\phi < 1$. For the case where the equilibrium P_3 or $\overline{P}_3$ collides with Σ, a Σ-node bifurcation occurs and the pseudo-equilibrium $PN \in \Sigma_1^s$. Note that regardless of the parameter conditions in the discontinuous model (1.6), same as models (1.2) and (1.3), there are no limit cycles, so that both species could stabilize their growth over time. In addition, a sliding segment is formed in the discontinuous model (1.6) regardless of the alteration of its parameters, so there are trajectories that slide along the sliding segment and converge to equilibrium or pseudo-equilibrium.

Comparing the models (1.2) and (1.3) with the discontinuous model (1.6), we have that the bifurcation cases for the models (1.2) and (1.3) are added to the bifurcations in the discontinuous model (1.6) whenever $s - qE > 0$ and P_3, or $\overline{P}_3$, is the unique interior equilibrium in the discontinuous model (1.6), that is, when $x_1 < M$, or $1 < \phi$ and $M < \overline{x}$, which guarantees that both species subsist over time. Furthermore, if P_3 is the only equilibrium in the discontinuous model (1.6), then the population size of prey is below the critical value $M > 0$. Similarly, if $\overline{P}_3$ is the only interior equilibrium, then the population size of prey is above the critical value $M > 0$. However, if $s - qE > 0$, $\phi < 1$ and $x_1 > M$,
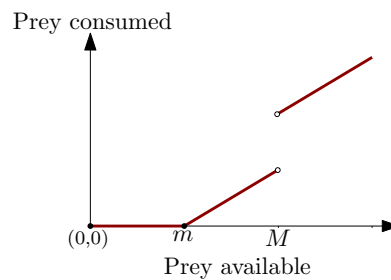
Figure 9. Predator functional response in the discontinuous model (1.6).

we have that PN exists, so the population size of prey converges to the critical value M. Similarly, if $s - qE > 0$, $1 < \phi$, $x_1 > M$ and $\overline{x} < M$, then P_3 and $\overline{P}_3$ are not interior equilibriums in the discontinuous model (1.6), so the population size of prey converges to the critical value $M > 0$.

Note that the predator functional response described in the discontinuous model (1.6), shown in Figure 9, could be viewed as a kind of sigmoid, or Holing III type, if we ignore the discontinuity at $x = M$. Although predator-prey models with Holing III predator functional response have limit cycles [35, 36], it does not give guarantee to assume the existence of limit cycles in the discontinuous model (1.6). A possible formation of limit cycles in Filippov systems arises from the existence of limit cycles in one of the conforming vector fields, together with the possible collision of these limit cycles with the sliding segment Σ^s, or cycles crossing Σ^c, as observed in Figure 2. Similarly, and naturally for continuous dynamical systems, the existence of at least one stable limit cycle could be deduced when all equilibriums of the discontinuous model are unstable [26, 29].

For the case where all prey take refuge from the predator when they are below the threshold value $M > 0$, the predators cannot consume the prey and the discontinuous model (1.6) is re-formulated by

$$\overline{V}(x, y) : \begin{cases} \dot{x} = rx\left(1 - \dfrac{x}{K}\right) - a\epsilon xy \\ \dot{y} = sy\left(1 - \dfrac{y}{n\epsilon x + c}\right) - qEy, \end{cases} \tag{7.1}$$

where

$$\epsilon = \begin{cases} 1, & \text{if } x > M, \\ 0, & \text{if } x < M, \end{cases}$$

of which has a single tangent point $\overline{T}$ and a stable pseudo-equilibrium PN. Moreover, the bifurcation cases are equivalent to that shown in Figure 8(a), in which region IV is interposed over regions V and VI, so that there are only 4 different behaviors in the dynamics between prey and predators. In this case and independent of the alterations on the parameters in the discontinuous model (7.1), the population size of prey could not be below the critical value $M > 0$ and the predators would lead to extinction if $s - qE < 0$.

Similarly, if there are a population size of prey $m > 0$ that is refuged from the predator at all times, the predator, upon consuming the remaining prey, must subsist solely on alternative food provided by the environment. Thus, the discontinuous model (1.6) is modified by:

$$\tilde{V}(x, y) : \begin{cases} \dot{x} = rx\left(1 - \dfrac{x}{K}\right) - a\epsilon(x - m)y \\ \dot{y} = sy\left[1 - \dfrac{y}{n\epsilon(x - m) + c}\right] - qEy, \end{cases} \tag{7.2}$$

where

$$\epsilon = \begin{cases} 1, & \text{if } x > m, \\ 0, & \text{if } x < m, \end{cases}$$

and the bifurcation cases are equivalent to those shown in Figure 4. Unlike the model (1.3), the discontinuous model (7.2) does not provide any constraint with respect to the behavior between the initial prey population size and quantity of prey refuges, i.e., $m < x(0)$ or $x(0) > m$.

Acknowledgments

Conflict of interest

The author declare there is no conflict of interest.

References

1. Y. A. Kuznetsov, *Elements of applied bifurcation theory*, Springer Press, New York, NY, USA, 2013. https://doi.org/10.1007/978-1-4757-3978-7

2. P. H. Leslie, J. C. Gower, The properties of a stochastic model for the predator-prey type of interaction between two species, *Biometrica*, **47** (1960), 219–234. https://doi.org/10.2307/2333294

3. N. Zhang, F. Chen, Q. Su, T. Wu, Dynamic behaviors of a harvesting Leslie-Gower predator-prey model, *Discrete Dyn. Nat. Soc.*, **2011** (2011), 473949. https://doi.org/10.1155/2011/473949

4. E. González-Olivares, C. Arancibia-Ibarra, A. Rojas, B. González-Yañez, Dynamics of a modified Leslie-Gower predation model considering a generalist predator and the hyperbolic functional response, *Math. Biosci. Eng.*, **16** (2019), 7995–8024. https://doi.org/10.3934/mbe.2019403

5. Q. Lin, C. Liu, X. Xie, Y. Xue, Global attractivity of Leslie-Gower predator-prey model incorporating prey cannibalism, *Adv. Differ. Equations*, **2020** (2020), 1–15. https://doi.org/10.1186/s13662-020-02609-w

6. E. Rahmi, I. Darti, A. Suryanto, A sodified Leslie-Gower model incorporating Beddington-DeAngelis functional response, double Allee effect and memory effect, *Fractal and Fractional*, **5** (2021), 84. https://doi.org/10.3390/fractalfract5030084

7. A. Arsie, C. Kottegoda, C. Shan, A predator-prey system with generalized Holling type IV functional response and Allee effects in prey, *J. Differ. Equations*, **309** (2022), 704–740. https://doi.org/10.1016/j.jde.2021.11.041

8. C. Arancibia-Ibarra, The basins of attraction in a modified May-Holling-Tanner predator-prey model with Allee affect, *Nonlinear Anal.*, **185** (2019), 15–28. https://doi.org/10.1016/j.na.2019.03.004

9. F. Chen, L. Chen, X. Xie, On a Leslie-Gower predator-prey model incorporating a prey refuge, *Nonlinear Anal. Real World Appl.*, **10** (2009), 2905–2908. https://doi.org/10.1016/j.nonrwa.2008.09.009

10. Q. Yue, Dynamics of a modified Leslie-Gower predator-prey model with Holling-type II schemes and a prey refuge, *SpringerPlus*, **5** (2016), 1–12. https://doi.org/10.1186/s40064-016-2087-7

11. S. Chen, W. Li, Z. Ma, Analysis on a modified Leslie-Gower and holling-type II predator-prey system incorporating a prey refuge and time delay, *Dyn. Syst. Appl.*, **27** (2018), 397–421. https://doi.org/10.12732/dsa.v27i2.12

12. U. Das, T. K. Kar, U. K. Pahari, Global dynamics of an exploited prey-predator model with constant prey refuge, *Int. Scholarly Res. Not.*, **2013** (2013), 637640. https://doi.org/10.1155/2013/637640

13. G. Tang, S. Tang, R. Cheke, Global analysis of a Holling type II predator-prey model with a constant prey refuge, *Nonlinear Dyn.*, **76** (2014), 635–647. https://doi.org/10.1007/s11071-013-1157-4

14. E. González-Olivares, R. Ramos-Jiliberto, Dynamic consequences of prey refuges in a simple model system: more prey, fewer predators and enhanced stability, *Ecol. Modell.*, **166** (2003), 135–146. https://doi.org/10.1016/S0304-3800(03)00131-5

15. Y. Kuznetsov, S. Rinaldi, A. Gragnani, One-parameter bifurcations in planar Filippov systems, *Int. J. Bifurcation Chaos*, **13**, (2003), 2157–2188. https://doi.org/10.1142/S0218127403007874

16. M. Guardia, T. M. Seara, M. A. Teixeira, Generic bifurcations of low codimension of planar Filippov Systems, *J. Differ. Equations*, **250** (2010), 1967–2023. https://doi.org/10.1016/j.jde.2010.11.016

17. J. Delcourt, P. Poncin, Shoals and schools: back to the heuristic definitions and quantitative references, *Rev. Fish Biol. Fish.*, **22** (2012), 595–619. https://doi.org/10.1007/s11160-012-9260-z

18. V. V. Isaeva, Self-organization in biological systems, *Biol. Bull.*, **39** (2012), 110–118. https://doi.org/10.1134/S1062359012020069

19. V. Křivan, A. Sikder, Optimal foraging and predator-prey dynamics, II, *Theor. Popul Biol.*, **55** (1999), 111–126. https://doi.org/10.1006/tpbi.1998.1399

20. B. O. Ma, P. A. Abrams, C. E. Brassil, Dynamic versus instantaneous models of diet choice, *Am. Nat.*, **162** (2003), 668–684. https://doi.org/10.1086/378783

21. V. Křivan, Behavioral refuges and predator-prey coexistence, *J. Theor. Biol.,* **339** (2013), 112–121. https://doi.org/10.1016/j.jtbi.2012.12.016

22. T. K. Kar, Stability analysis of a prey-predator model incorporating a prey refuge, *Commun. Nonlinear Sci. Numer. Simul.*, **10** (2005), 681–691. https://doi.org/10.1016/j.cnsns.2003.08.006

23. D. Jana, Stabilizing effect of prey refuge and predator's interference on the dynamics of prey with delayed growth and generalist predator with delayed gestation, *Int. J. Ecol.*, **2014** (2014), 429086. https://doi.org/10.1155/2014/429086

24. D. Jana, R. Agrawal, R. K. Upadhyay, Dynamics of generalist predator in a stochastic environment: effect of delayed growth and prey refuge, *Appl. Math. Comput.*, **268** (2015), 1072–1094. https://doi.org/10.1016/j.amc.2015.06.098

25. J. Yang, S. Tang, R. A. Cheke, Global stability and sliding bifurcations of a non-smooth Gause predator-prey system, *Appl. Math. Comput.*, **224** (2013), 9–20. https://doi.org/10.1016/j.amc.2013.08.024

26. C. Cortés García, Bifurcaciones en Modelo Gause Depredador-Presa con discontinuidad, *Rev. Mat*, **28** (2021), 183–208. https://doi.org/10.15517/rmta.v28i2.36084

27. A. A. Arafa, S. A. Hamdallah, S. Tang, Y. Xu, G. M. Mahmoud, Dynamics analysis of a Filippov pest control model with time delay, *Commun. Nonlinear Sci. Numer. Simul.*, **101** (2021), 105865. https://doi.org/10.1016/j.cnsns.2021.105865

28. C. C. García, Bifurcations in discontinuous mathematical models with control strategy for a species, *Math. Biosci. Eng.*, **19** (2021), 1536–1558. https://doi.org/10.3934/mbe.2022071

29. C. C. García, Bifurcations on a discontinuous Leslie-Grower model with harvesting and alternative food for predators and Holling II functional response, *Commun. Nonlinear Sci. Numer. Simul.*, **116** (2023), 106800. https://doi.org/10.1016/j.cnsns.2022.106800

30. R. P. Dunn, K. A. Hovel, Predator type influences the frequency of functional responses to prey in marine habitats, *Biol. Lett.*, **16** (2020), 20190758. https://doi.org/10.1098/rsbl.2019.0758

31. J. Sotomayor, *Lições de equações diferenciais ordinárias*, IMPA Press, Rio de Janeiro, 1979.

32. D. Jana, S. Ray, Impact of physical and behavioral prey refuge on the stability and bifurcation of Gause type Filippov prey-predator system, *Model. Earth Syst. Environ.*, **2** (2016), 24. https://doi.org/10.1007/s40808-016-0077

33. W. Li, J. Ji, L. Huang, J. Wang, Bifurcations and dynamics of a plant disease system under non-smooth control strategy, *Nonlinear Dyn.*, **99** (2020), 3351–3371. https://doi.org/10.1007/s11071-020-05464-2

34. W. Li, J. Ji, L. Huang, Dynamics of a controlled discontinuous computer worm system, *in Proceedings of the American Mathematical Society*, AMS, **148** (2020), 4389–4403. https://doi.org/10.1090/proc/15095

35. A. A. Shaikh, H. Das, N. Ali, Study of a predator-prey model with modified Leslie-Gower and Holling type III schemes, *Model. Earth Syst. Environ.*, **4** (2018), 527–533. https://doi.org/10.1007/s40808-018-0441-1

36. E. González-Olivares, P. C. Tintinago-Ruiz, A. Rojas-Palma, A Leslie-Gower-type predator-prey model with sigmoid functional response, *Int. J. Comput. Math.*, **92** (2015), 1895–1909. https://doi.org/10.1080/00207160.2014.889818

AIMS Press